J. Coat. Technol. Res., **19** (4) 1087–1100, 2022
https://doi.org/10.1007/s11998-021-00587-6

Enhanced anticorrosion property of epoxy resin membrane by nano-organic montmorillonite

Jing-yi Liu, Shi-zhao Wu, Zhu Shen, Jing Gao, Xin-quan Hu, Guo-hua Li

Received: 10 March 2021 / Revised: 11 November 2021 / Accepted: 20 November 2021

Abstract Montmorillonite (Mnt) and organic polymer composite membrane are widely used to enhance the corrosive resistance of metal materials due to their unique properties. Herein, a uniform anticorrosion membrane coated on aluminum plate was fabricated with organic-modified nano-Mnt (OMnt) and epoxy resin (EP) as raw materials, which showed good smoothness, wear property and resistance to acidic and salty corrosion. The surface morphology, crystal phase, chemical composition, and microstructure of the OMnt/EP membrane were characterized by optical microscopy, small-angle X-ray diffraction, FTIR, SEM, and TEM, respectively. The results showed that the OMnt/EP membrane was constituted of OMnt and EP. The interplanar distance of OMnt was expanded from 1.44 to 5.36 nm. Electrochemical corrosive resistance of the membrane was tested with Tafel polarization curves and electrochemical impedance spectroscopy. The results showed that the thickness of the membrane had a positive effect on its anticorrosion performance. When its thickness was 0.18 mm, its corrosion voltage (P_{corr}) increased along with its content of OMnt, while its corrosion current (I_{corr}) showed increasing, decreasing and increasing trend as the content increased from 1 to 5%, from 5 to 7% and from 7 to 9%, respectively. When its content of OMnt was the same, its P_{corr} increased along with its thickness, while its I_{corr} decreased along with its thickness. Its maximum impedance reached 2.29×10^7 Ω, which was much greater than that of other EP membranes. Moreover, the corrosion resistance of the composite membranes decreased gradually as the immersion time increased, and the content of OMnt and the ratio of EP to OMnt could also affect the corrosion resistance of the membrane. These results show that the OMnt/EP composite membrane exhibits excellent anticorrosive property, which is highly promising for wide applications in industry.

Keywords Organic montmorillonite, Epoxy resin, Composite membrane, Enhancement, Anticorrosive property

J. Liu, S. Wu, Z. Shen, J. Gao, X. Hu, G. Li (✉)
School of Chemical Engineering, Zhejiang University of Technology, Hangzhou 310014, People's Republic of China
e-mail: nanozjut@zjut.edu.cn

J. Gao, X. Hu, G. Li
State Key Breeding Base of Green Chemistry Synthesis Technology, Hangzhou 310014, People's Republic of China

Introduction

Metal corrosion has become one of the major causes of damage to metal materials, which results in a great many accidents and aggravates environmental pollution, leading to huge economic loss and retarded development of high-technology.[1] According to the estimated results, the economic loss caused by metal corrosion is about 3–5% of the total GDP all over the world each year. For example, the total GDP of China was about 99.09 trillion yuan, and the economic loss caused by metal corrosion was 2.97–4.95 trillion yuan in 2019. So, the surface protection of metal materials has become a hot research topic today.[2–4]

Aluminum plate has been widely used in sports, aerospace, transportation, and civil industry due to its good ductility, low specific gravity, and low density. However, its corrosion resistance is not high.[5,6] Traditionally, corrosion inhibitors, chromate passivation, and anodic oxidation are three efficient ways to enhance the corrosion performance of aluminum. Though the chromate passivation process is simple, hexavalent chromium is harmful to human body and environment.[7,8] The anodic oxidation process is complex and expensive, of which the obtained anodic oxide film exhibits high hardness and brittle texture.[9,10]

Therefore, it is necessary to develop an anticorrosion coating with simple process, low cost, environmental friendliness, and excellent performance.

Montmorillonite (Mnt) and organic polymer composite membrane are widely used to enhance the corrosion resistance of metal materials due to their unique properties. Nano-Mnt has good performance in improving the anticorrosion and barrier properties of pure epoxy resin (EP) due to its environmental friendliness.[11,12] Therefore, organics modified Mnt was used as raw material to composite with organic polymer to fabricate membrane for protecting aluminum plate.[13]

The organic coating has high ion resistance and sets up a good barrier to prevent the diffusion of chemical substances, such as water, ions, or oxygen, into the metal surface, thereby greatly reducing the corrosion rate of aluminum.[14] In this paper, organic nano-Mnt (OMnt) was exploited to fabricate an OMnt/EP composite membrane to enhance the anticorrosion performance of aluminum.[15–17] The organic nano-Mnt (OMnt) was obtained by organic modification of sodium-based Mnt. The highlight of this paper is to add OMnt nanoparticles into EP to eliminate defects and voids among EP molecules during the coating and curing process of the membrane, and to prevent EP from decomposing during the curing process; thus, the corrosion resistance, the interphase adhesion as well as mechanical strength[18–20] between the membrane and aluminum surface can be enhanced.

Experimental and characterization

Chemical regents and materials

Aluminum plate (size 100 mm × 15 mm × 1 mm), alkaline sodium-based Mnt (Xincheng Mineral Products Co., Ltd.), Tween 20 and 80 (Aladdin Reagent Company), hexadecylamine (Aladdin Reagent Company), silane coupling agent KH-550 (Nanjing Genesis Chemical Additives Co., Ltd.), epoxy resin E51 (Baling Petrochemical Company), active diluent 669 (Wuxi Qianguang Chemical Raw Materials Co., Ltd.), curing agent: low molecular polyamide 650 (Danbao Resin Co., Ltd.), promoter: DMP-30 (2, 4, 6-tris(dimethylaminomethyl)phenol, Changzhou Runxiang Chemical Co., Ltd.). All the chemical regents and materials aforementioned were used directly without any further treatment.

Cation exchange capacity (CEC) of Mnt

The pH value of natural Mnt is 9-10, and its cation exchange capacity (CEC) was measured by NH_4Cl-ethanol method. First, 1 g of Mnt powder was dispersed into 25 mL of ethanol aqueous solution under stirring. After 5 min, the Mnt suspension was centrifuged at a speed of 8000 r/min for 8 min. The precipitate was collected to repeat the above dispersion and centrifuging process for another two cycles. Then, the precipitate was dispersed in a mixed aqueous solution (0.1 mol/L NH_4Cl and 70 (v/v)% ethanol) and then stirred for 30 min. The suspension was then left for 24 h before being centrifuged. The precipitate with 25 mL of H_2O, 8 mL of formaldehyde and 3–4 drops of phenolphthalein solution were titrated with 1 mol/L NaOH. The consumed volume of NaOH solution was recorded as V_1. The above titration process was repeated three times to get an average value of V_1. Similar titration procedures were performed on a mixed aqueous solution composed of 0.1 mol/L NH_4Cl and 70 (v/v)% ethanol and the average consumed volume of NaOH was marked as V_2. The CEC of Mnt can be estimated according to the following formula:

$$\mathrm{CEC} = \frac{(V_2 - V_1) \times C \times 100\,(\text{total volume of exchange capacity})}{\text{sample weight} \times \text{titration volume (25 mL)}}$$

where C stands for the concentration of the mixed NH_4Cl/ethanol aqueous solution. The CEC of high-quality bentonite is 115–139 mmol/100 g. The larger the CEC of Mnt, the stronger its hydration, expansion and dispersion capabilities are. Based on the above calculation, the CEC of Mnt in our experiment was 126.48 mmol/100 g.

Organics modified nano-Mnt (OMnt)

First, 5 g of natural Mnt powder was dispersed into 500 mL deionized water, stirred for 120 min and ultrasonically dispersed for 30 min. The as-obtained suspension was marked as A. Next, 1.53 g of hexadecylamine (HDA), which was equivalent to 1.0 CEC of Mnt, was added into 50 mL of absolute ethanol under stirring to obtain suspension B. Then suspension A and B were mixed and stirred for 120 min in a water bath at 80°C to get suspension C, which was then centrifuged at a speed of 8000 r/min for 8 min. The precipitate was collected and washed by absolute ethanol and then ionic water until no precipitate formed in the waste liquid to which $AgNO_3$ was added. Then the precipitate was dried in an oven at 80°C overnight and ground to obtain OMnt.[21]

Preparation of OMnt/EP nanocomposite membrane

First, 50 g of epoxy resin (EP) and 7.5 g diluent 669 were mechanically stirred to get a mixture, to which 0.5–4.5 g of OMnt powder was added. After 2 h of stirring in a water bath at 80°C followed by 1 h of ultrasonication, mixture A was obtained. Then, 25 g of polyamide 650 as curing agent was diluted in acetone at a mass ratio of 1: 1 (polyamide 650 to acetone) to obtain mixture B, which was then added into mixture

A to obtain mixture C. In order to shorten curing time of mixture C, 2.5 g of DMP-30 as curing accelerator was added followed by 30 min mechanical stirring and 30 min ultrasonication. Then several drops of defoamer were added into mixture C, which formed a mixed paste of OMnt and EP after 30 min. The mixed paste was coated on the surface of aluminum plate pretreated with a brush and a scraper, which finally formed an OMnt/EP composite membrane.[22,23]

Characterization

X-ray diffractometer (X'Pert PRO, PANalytical Co.) was performed at a voltage of 40 kV and a current of 40 mA, using Cu Ka as an incident light source with a scanning rate of 2.4 °/min and a step length of 0.04°. Fourier-transform infrared spectrometer (Nicolet 6700, American Thermoelectric Nichols Co.) was carried out with a range from 400 to 4000 cm^{-1} after the samples were pressed into pellets with KBr. Field-emission scanning electron microscope (S24700, Hitachi Co.) and high-resolution transmission electron microscope (Tecnai G2 F30, Philips-FEI Co.) were performed at a voltage of 15 kV and 200 kV, respectively. Video optical contact angle measuring instrument (OCA-20, Dataphysics Co.) was used to measure the contact angles of Mnt before and after organic modification.

Electrochemical performance

CHI 660E electrochemical workstation was used to test Tafel polarization curve with a scanning potential range of 0.2∼ −1.4 V and 0∼ −1.2 V at a sweep rate of 3 mV/s, and AC impedance test (EIS) with a frequency range of 0.1–10^5 Hz.[24] Before the test, the aluminum plate coated with OMnt/EP membrane was immersed in a mixed aqueous solution (1.0 mol/L NaCl and 0.5 mol/L H_2SO_4 with volume ratio of x) for 30 min to reach an adsorption and desorption equilibrium. During the test, a three-electrode system was used to measure the anticorrosive property of the OMnt/EP membrane in 1.0 mol/L NaCl solution. The aluminum plate coated with OMnt/EP membrane, an Ag/AgCl electrode and platinum electrode were used as working electrode (WE), reference electrode (RE), and counter electrode (CE), respectively.

Results and discussion

XRD

In order to investigate the interlayer space of Mnt before and after organics modification, X-ray small-angle diffraction tests were carried out for Na-Mnt and organics modified Mnts, respectively (Fig. 1). The organic compounds used for modifying Mnt included

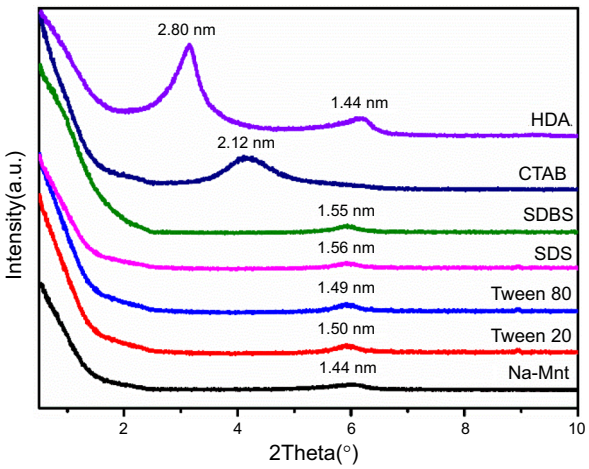

Fig. 1: XRD patterns of Mnts with different modifiers

Tween 20 (T20), Tween 80 (T80), sodium dodecyl sulfate (SDS), sodium dodecyl benzene sulfonate (SDBS), cetyl trimethyl ammonium bromide (CTAB), and hexadecylamine (HDA). In Fig. 1, the characteristic diffraction peak of (001) with 2θ at 6.102° of Na-Mnt can be clearly observed, of which the interlayer space $d_{(001)}$ was 1.44 nm according to the Bragg Equation. After being modified by nonionic surfactants, T20 and T80, the (001) diffraction peak of Mnt shifted to 2θ at 5.924° and 5.936°, respectively, of which the $d_{(001)}$ was 1.50 nm and 1.49 nm, respectively. Similarly, the (001) diffraction peak of Mnt modified by anionic surfactants, SDS and SDBS, was at 2θ of 5.707° and 5.709°, respectively, and their corresponding $d_{(001)}$ was 1.56 nm and 1.55 nm, respectively. Compared to $d_{(001)}$ of Na-Mnt, the $d_{(001)}$ values of Mnts modified by T20, T80, SDS, and SDBS showed limited increase.

For Mnt modified by cationic surfactants, CTAB and HDA, their diffraction peaks (001) were at 2θ of 4.163° and 3.151°, respectively, corresponding to $d_{(001)}$ of 2.12 nm and 2.80 nm, respectively. These $d_{(001)}$ values were much larger than that of Na-Mnt (1.44 nm), which can be attributed to the reason that CTAB and HDA are cationic surfactants that could replace Na^+ and Ca^{2+} in the interlaminar space of Mnt by cation exchange, thus increasing the interlayer distance of Mnt. It should be noticed that $d_{(001)}$ of Mnt modified by CTAB was smaller than that of Mnt modified by HDA, which may be due to insufficient cation exchange or the influence from organic intercalants. In detail, Mnt modified by HDA exhibits two diffraction peaks with interlayer distances of 2.80 nm and 1.44 nm, respectively, yet the intensity of its second diffraction peak was relatively weak (Fig. 1), indicating that part of the interlayers of Mnt may not be inserted by HDA during the modification.

The effects of reaction temperature, time, and pH value and the content of HDA on the increase of the interlayer distance of HDA-modified Mnt were investigated and the results are shown in Fig. 2. During the

modification, regardless of the reaction time length, all the Mnt samples exhibited two diffraction peaks with almost the same diffraction angle, of which the corresponding interlayer distances were 2.82 nm and 1.43 nm, respectively (Fig. 2a), suggesting that the reaction time is not the key factor affecting the interlayer distance of HDA-modified Mnt. The influences of reaction temperature showed similar results when at 50, 60, 70, and 90°C. When the reaction temperature was 80°C, the interlayer distance of the first peak was 2.77 nm, which is within the error range of 2.82 nm, and the second peak is almost nonexistent, indicating that Mnt was basically intercalated by HDA (Fig. 2b). Wang et al.[25] reported that the optimal reaction temperature for organic modification of Mnt was 70–80°C, and if the temperature was too high, the ion exchange capacity of Mnt decreased. Therefore, the reaction temperature was set as 70°C in later organic modification of Mnt.

The influence of pH value on the modification of Mnt was explored. When the pH value of reaction solution was between 1 and 3, only one diffraction peak with a broad range appeared in XRD patterns of the HDA-modified Mnt, as shown in Fig. 2c. The reason might be that under this condition the cation exchange reaction was inhibited due to high concentration of H^+. When pH was higher than 5, two diffraction peaks can be observed in XRD patterns of HDA-modified Mnts (Fig. 2c). For the first diffraction peak, its corresponding interlayer distance increased along with the pH value, while that of the second diffraction peak had no change (Fig. 2c). When the content of HDA used in modification was equivalent to 0.2–0.6 CEC, the modified Mnt exhibit only one diffraction peak and its corresponding interlayer distance increased along with the content of HDA (Fig. 2d). When the content of HDA used in modification was equivalent to 0.8–1.0 CEC, the modified Mnt exhibited two diffraction peaks. As the content of HDA increased, the corresponding interlayer distance of the first peak varied from 2.76 to 2.85 nm while that of the second peak was stable at 1.44 nm (Fig. 2d). When the content of HDA was higher than 1.5 CEC, the modified Mnt showed three diffraction peaks and the interlayer distance for

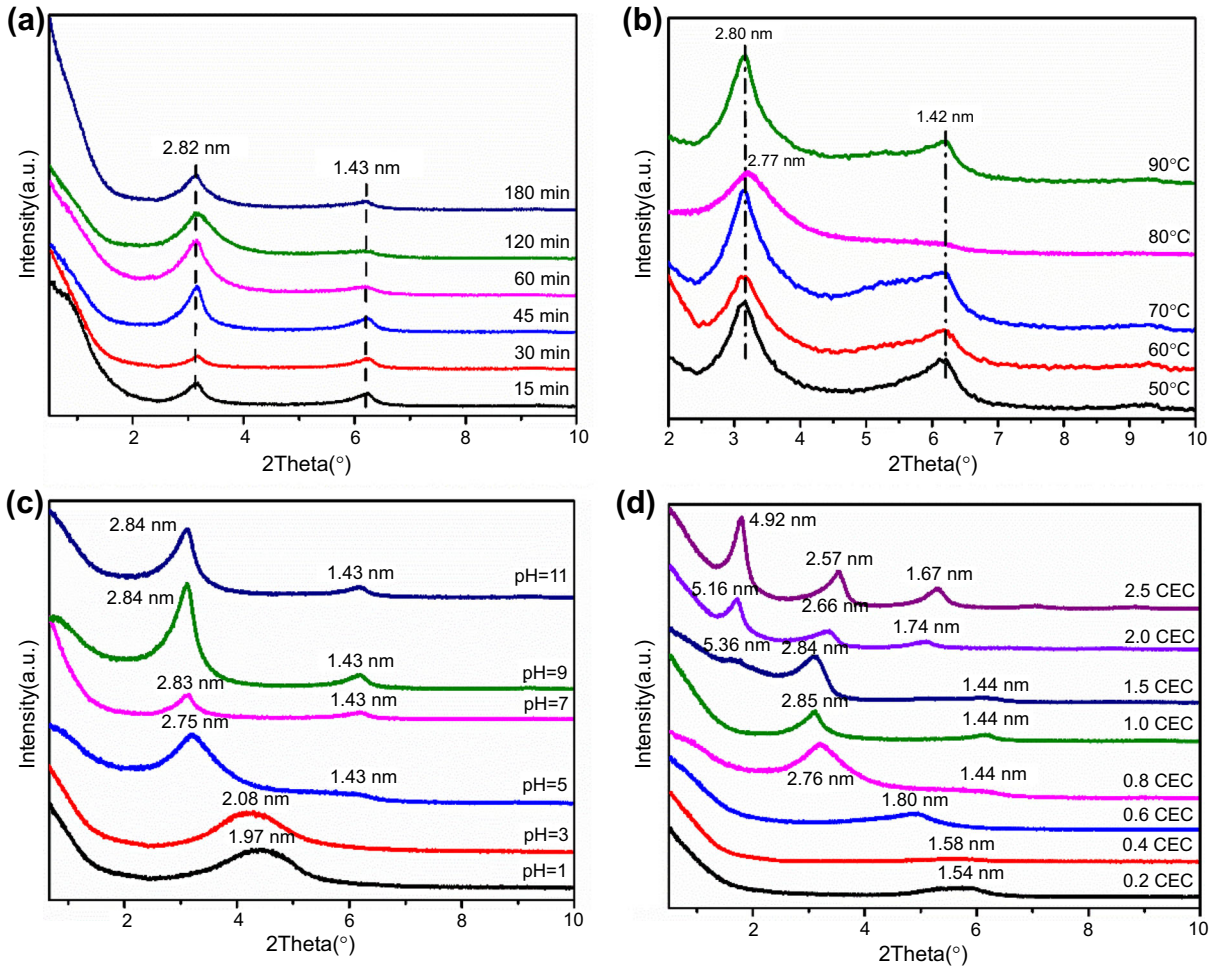

Fig. 2: XRD patterns of Mnts modified by HDA for different time (a), at different temperature (b), under different pH value (c), and with different HDA contents (d)

each diffraction peak was marked in Fig. 2d, which showed that the interlayer distance of Mnts began to decrease when the content of HDA was more than 1.5 CEC. The reason might be that the content of HDA surpassed the exchange ability of Mnt, resulting in excessive HDA molecules intercalating into the interlayers of Mnt. When the content of HDA was lower than 0.6 CEC, only one peak appears, and the interlayer distance gradually increased with the increase of the amount of HDA. This is because when the amount of HDA was small, almost all of them were intercalated into the Mnt layer, thus the interlayer distance is larger than 1.44 nm. As the content of HDA increased, a lot of foams appeared during the reaction. These foams inhibited the ion exchange reaction between HDA and Mnt, causing low efficiency of HDA modification. As a result, the content of HDA is a critical factor that affects the interlayer distance of HDA-modified Mnt.

SEM

SEM image of Na-Mnt is shown in Fig. 3, indicating a limited dispersion of the Na-Mnt layers. After organic modification by T20, T80, SDS, or SDBS, the morphology and dispersion of Mnts did not change obviously (Fig. 4a, 4b, 4c, and 4d). The morphology and layer dispersion did not change neither for CTAB-modified Mnt, yet some layers curled at the edges (Fig. 4e). For HDA-modified Mnt, its morphology and dispersion changed significantly with obviously curled layer edges and its layer thickness was uniform as well (Fig. 4f).

Figure 5 shows SEM images of HDA-modified Mnt with different HDA content. The dispersion of HDA-modified Mnt improved along with the increase of HDA content. Besides, the curly phenomenon of the Mnt layers became more and more obvious as the HDA content increased. These results indicate that HDA was intercalated into the interlayers of Mnt rather than simply mixed with Mnt, especially when the content of HDA was higher than 1.5 CEC, which is consistent with that of the XRD results.

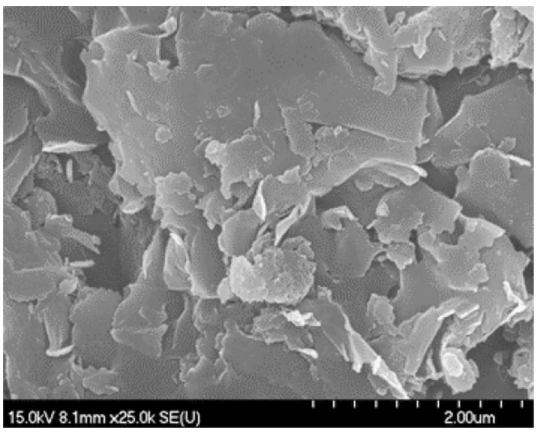

Fig. 3: SEM image of Na-Mnt

TEM

TEM image of Na-Mnt shows a lamellar structure with an interlayer distance of 1.44 nm (Fig. 6). After being modified by T20, T80, SDBS, or SDS, the lamellar structure and the interlayer distance of Mnt (1.49–1.56 nm) showed little change (Fig. 7a, 7b, 7c, and 7d). For CTAB and HDA-modified Mnt, their interlayer distance greatly increased to 2.12 and 2.80 nm, respectively (Fig. 7e and 7f). These results are in-line with that of XRD tests.

Figure 8 shows TEM images of HDA-modified Mnt with different HDA content. Based on these TEM images, the values of interlayer distance of each Mnt sample are summarized in Table 1. From Table 1 it can be seen that the interlayer distance varied significantly as the HDA content changed, confirming the key role of HDA content in affecting the interlayer distance of HDA-modified Mnt, which is also consistented with the XRD results.

Contact angle

In order to investigate the hydrophobicity of the surface of HDA-modified Mnt, contact angle tests at 0 s and 30 s for each sample were performed and the results are displayed in Fig. 9. For the tests at 0 s, the contact angle of the Mnt samples increased along with the HDA content, which showed similar trends for the tests at 30 s. For each sample, the contact angle tested at 0 s was a little larger than that tested at 30 s. It should also be pointed out that all the contact angles were larger than 90.0°, indicating that the hydrophilic surface of Mnt changed to hydrophobic after HDA modification, and the higher the HDA content, the more hydrophobic the surface of the HDA-modified Mnt.

FTIR

The Fourier-transform infrared spectra (FTIR) of Mnt, OMnt, EP, and OMnt/EP are shown in Fig. 10. Detailed analysis of the spectra is summarized in Table S1. The FTIR spectrum of OMnt exhibits all the characteristic peaks of HDA and Mnt Fig.10. Similarly, all the characteristic peaks of OMnt and EP can be observed in the FTIR spectrum of OMnt-EP, indicating that EP was successfully combined with OMnt, forming OMnt-EP composite membrane.

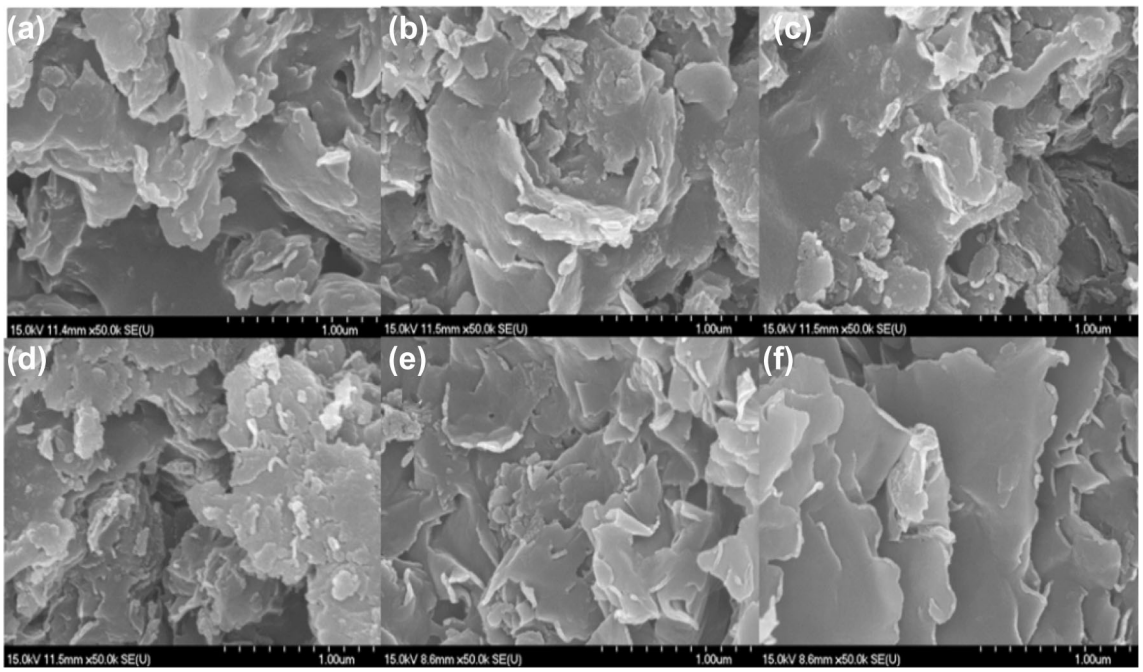

Fig. 4: SEM images of modified montmorillonite (a: T20, b: T80, c: SDS, d: SDBS, e: CTAB, f: HDA)

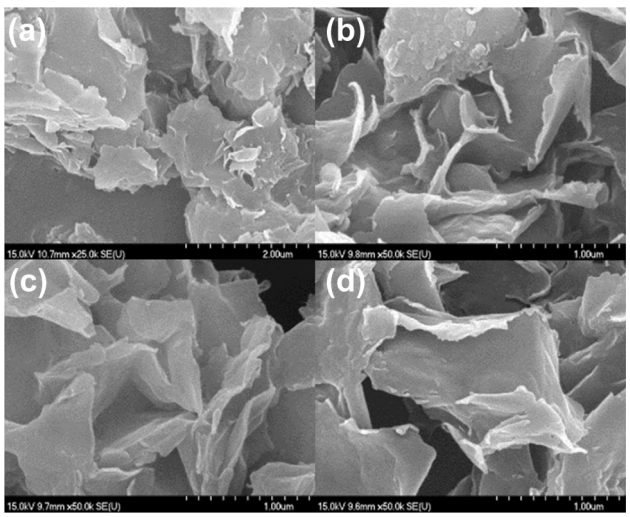

Fig. 5: SEM images of Mnt modified by HDA with different CEC (a: 1.0, b: 1.5 CEC, c: 2.0 CEC, d: 2.5 CEC)

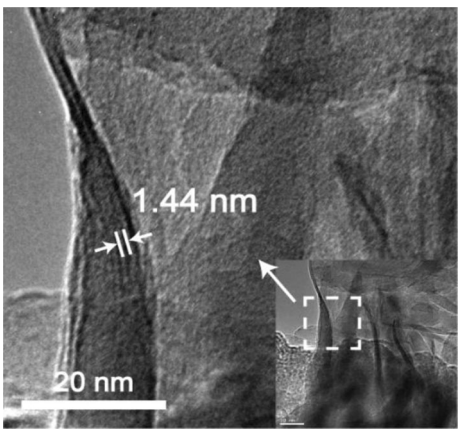

Fig. 6: TEM image of Na-Mnt

Tafel polarization curve

The Tafel polarization curves of aluminum plate and those coated with OMnt/EP composite membranes with different OMnt contents are shown in Fig. 11. Corrosion potential (P_{corr}) and current density (I_{corr}) for each sample are listed in Table 2.

The I_{corr} of pure EP (8.94×10^{-6} A cm^{-2}) was significantly reduced compared to that of the aluminum plate (6.76×10^{-5}), indicating that pure EP has anticorrosion property. Besides, regardless of the OMnt content, the P_{corr} of all the OMnt/EP membranes was more positive than that of the aluminum plate, while their I_{corr} values obviously decreased. In detail, the P_{corr} of the OMnt/EP membrane increased along with the OMnt content while the I_{corr} first increased as the OMnt content increased from 1 to 5%, then decreased as the OMnt content increased from 5 to 7%, and increased again as the OMnt content further increased to 9%. These results indicate that the addition of OMnt into EP can improve the anticorrosion performance and reduces its corrosion rate. Thus,

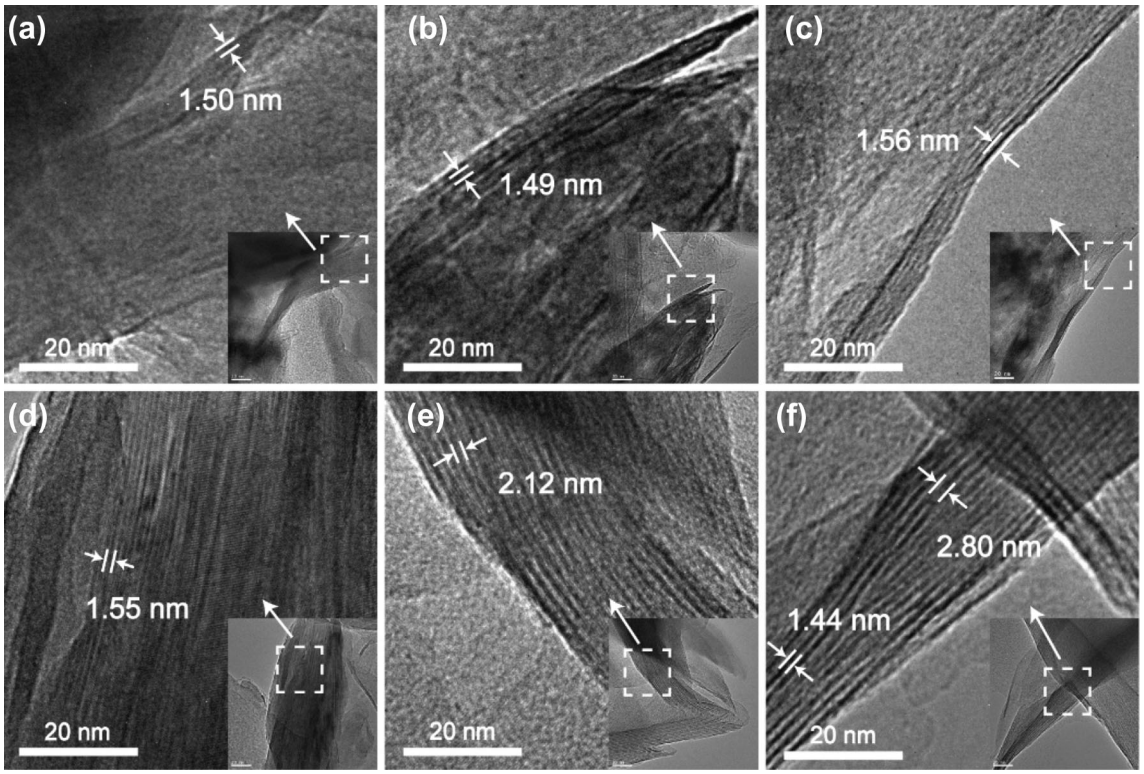

Fig. 7: TEM images of Mnt modified by different organics (a) T20, (b) T80, (c) SDS, (d) SDBS, (e) CTAB, and (f) HDA

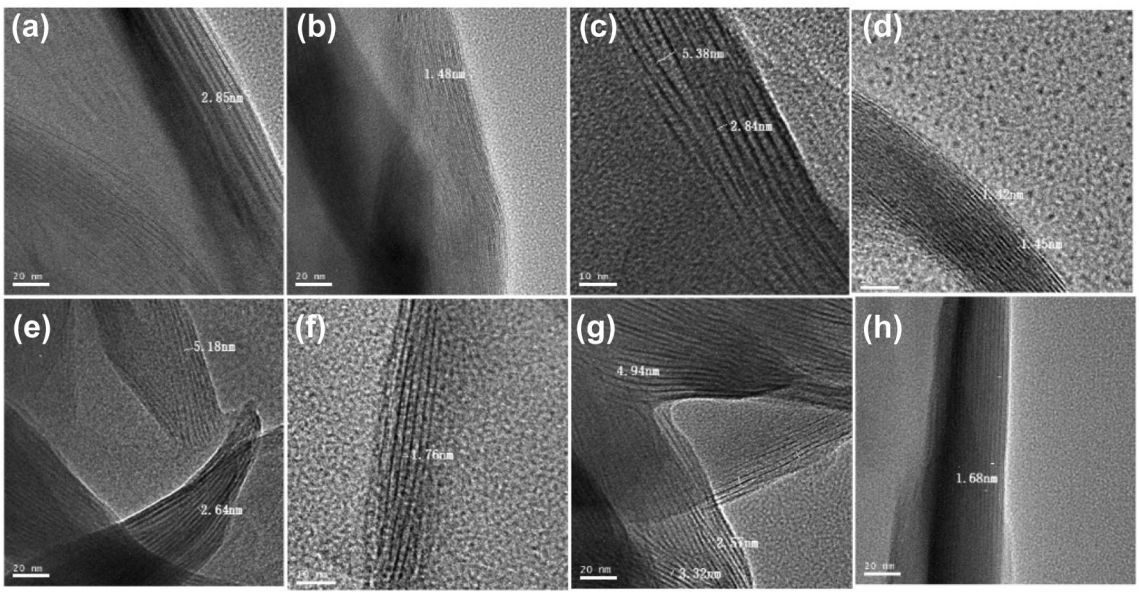

Fig. 8: TEM images of Mnt modified with different CEC of HDA (a, b: 1.0; c, d: 1.5; e, f: 2.0; g, h: 2.5)

the effect of OMnt thickness on anticorrosion performance of OMnt-EP membrane was investigated. Figures 11b, 11c, 11d, 11e, and 11f show the polarization curve of OMnt-EP membranes with the same OMnt content but different thicknesses, of which the corresponding values of P_{corr} and I_{corr} are also listed in Table 2. It can be concluded from Table 2 that the P_{corr} of the OMnt-EP membrane increased along with its thickness, while the I_{corr} decreased with increasing thickness, implying that the thickness of the membrane has a positive impact on its anticorrosion performance.

EIS

EIS curves of OMnt/EP composite membranes with different thicknesses and different OMnt contents are shown in Fig. 12a, 12b, 12c, 12d, and 12e, of which the corresponding impedance values are listed in Table 3. When OMnt contents of the membranes were the same, the impedance value increased significantly along with the thickness and the maximum impedance value could reach to 2.29×10^7 Ω, which was much greater than that of the other EP membranes. In addition, the impedance values of the Mnt-based coatings with two or three components are smaller than 10^7, as reported in references (23), (13), (12), and (5) (Table 4). The impedance value of OMnt-based coating with three components is slightly bigger than that reported in our work, as reported in reference (22) (Table 4). When nano-Mnt composited with multicomponent, the impedance value of the composite is much bigger than that of our work, as reported in reference (9) (Table 4). The reason might be OMnt can better combine with organic materials, such as EP and 2-BBI, than nonmodified Mnt does. Nano-sized Mnt exhibits much higher surface activity compared to its precursor, leading to enhanced binding force between nano-sized Mnt and epoxy resin. Therefore, organic modification and nanoscale Mnt can enhance anticorrosion ability of Mnt-based organic composite membranes.

When the OMnt content was only 1% and the thickness of the composite membrane was 0.08 mm, the EIS spectrum shows one resistance (Fig. 13a_1), which can be ascribed to main contribution from EP to the anticorrosion effect. As the OMnt content in-

Table 1: Interlayer distance of HDA-modified Mnt with different HDA content

Content of HDA	Interlayer distance (nm)		
1.0 CEC	1.48	2.85	
1.5 CEC	1.45	2.84	5.38
2.0 CEC	1.76	2.64	5.18
2.5 CEC	1.68	2.57	3.32

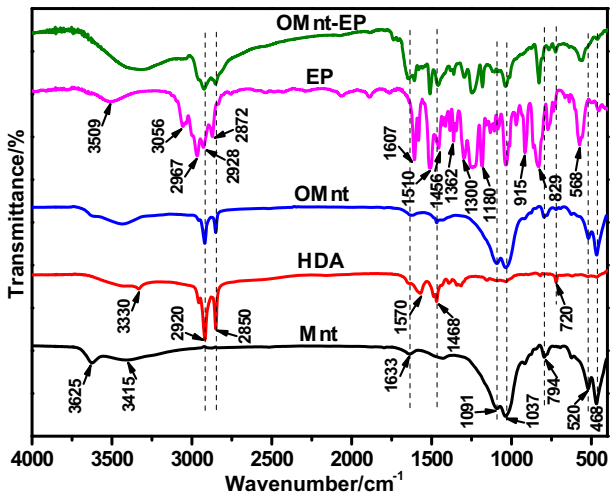

Fig. 10: FTIR spectra of EP, OMnt, and OMnt/EP

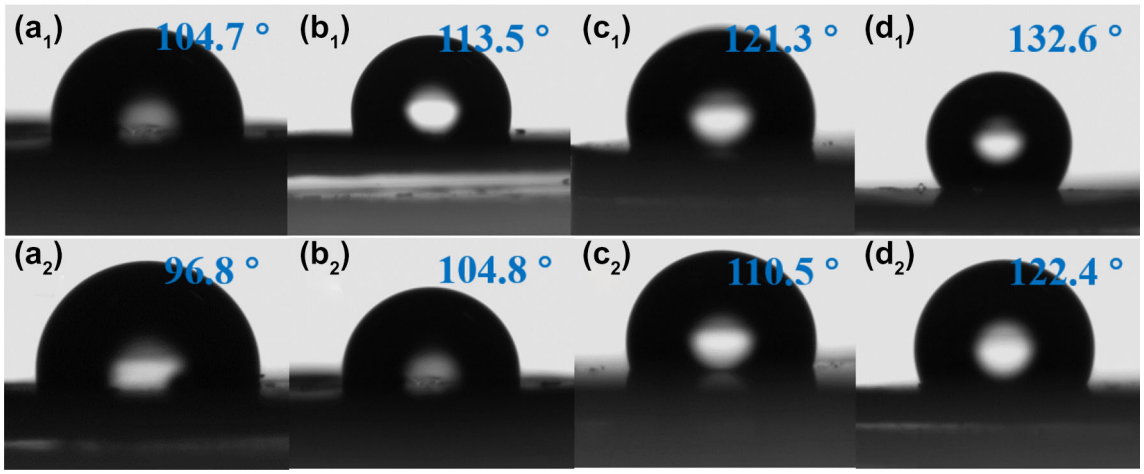

Fig. 9: Contact angles of Mnts modified with different HDA content Test at 0 s (a_1: 1.0 CEC; b_1: 1.5 CEC; c_1: 2.0 CEC; d_1: 2.5 CEC) and tests at 30 s (a_2: 1.0 CEC; b_2: 1.5 CEC; c_2: 2.0 CEC; d_2: 2.5 CEC)

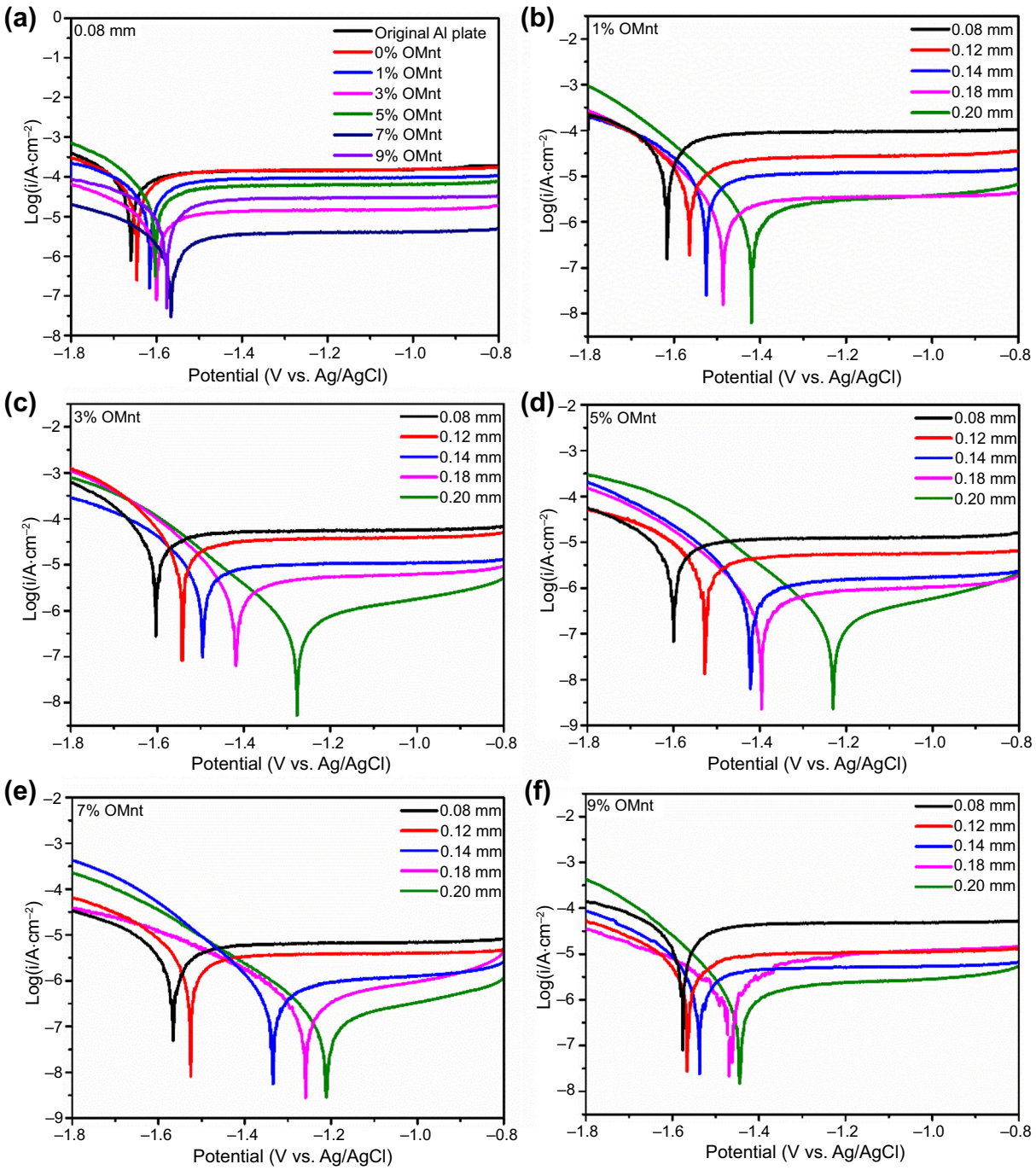

Fig. 11: Tafel polarization curves of composite membranes with different thicknesses and contents of OMnt

creased, two resistances can be observed in the EIS curves (Fig. 13a$_2$, 13a$_3$, and 13a$_4$), due to co-contribution to resistances from EP and OMnt. When the thickness of the composite membrane was 0.20 mm, one resistance displays in Fig. 13a$_5$, which can be attributed to a synergistic effect between EP and OMnt. When the amount of OMnt increased to a certain extent, OMnt reacted with EP, forming a uniform membrane texture, thus only one impedance value is shown in the EIS spectrum.

Table 2: P_{corr} and I_{corr} of OMnt/EP with different OMnt contents and thicknesses

Sample	Membrane thickness/mm	P_{corr}/V	I_{corr}/A	Sample	Membrane thickness/mm	P_{corr}/V	I_{corr}/A
1% OMnt/EP	0.08	−1.62	2.95×10^{-5}	5% OMnt/EP	0.18	−1.39	3.16×10^{-7}
1% OMnt/EP	0.12	−1.56	6.46×10^{-6}	5% OMnt/EP	0.20	−1.23	1.62×10^{-7}
1% OMnt/EP	0.14	−1.52	6.61×10^{-6}	7% OMnt/EP	0.08	−1.58	2.63×10^{-6}
1% OMnt/EP	0.18	−1.48	4.07×10^{-6}	7% OMnt/EP	0.12	−1.52	1.66×10^{-6}
1% OMnt/EP	0.20	−1.42	4.79×10^{-7}	7% OMnt/EP	0.14	−1.33	4.07×10^{-7}
3% OMnt/EP	0.08	−1.60	1.86×10^{-5}	7% OMnt/EP	0.18	−1.26	1.18×10^{-7}
3% OMnt/EP	0.12	−1.54	1.55×10^{-5}	7% OMnt/EP	0.20	−1.21	8.32×10^{-8}
3% OMnt/EP	0.14	−1.49	4.90×10^{-6}	9% OMnt/EP	0.08	−1.58	1.78×10^{-5}
3% OMnt/EP	0.18	−1.42	2.29×10^{-6}	9% OMnt/EP	0.12	−1.56	4.17×10^{-6}
3% OMnt/EP	0.20	−1.28	8.71×10^{-7}	9% OMnt/EP	0.14	−1.54	2.19×10^{-6}
5% OMnt/EP	0.08	−1.60	4.78×10^{-6}	9% OMnt/EP	0.18	−1.46	1.62×10^{-6}
5% OMnt/EP	0.12	−1.53	2.24×10^{-6}	9% OMnt/EP	0.20	−1.44	5.37×10^{-7}
5% OMnt/EP	0.14	−1.42	6.61×10^{-7}				

When the content of OMnt was 3%, the experiment results (Fig. 13b_1, 13b_2, 13b_3, and 13b_4) were similar to that with OMnt content of 1% (Fig. 13a_1, 13a_2, 13a_3, and 13a_4), except two resistances are shown in Fig. 13b_5. This difference can be attributed to the increased content of OMnt for Fig. 13b_5 compared to that for Fig. 13a_5. In this case, both EP and OMnt played the anticorrosion effect.

When the content of OMnt increased to 5%, the experiment results (Fig. 13c_1, 13c_3, 13c_4, and 13c_5) were similar to that with OMnt content of 3% with one difference in Fig. 13c_2. The experiment results for OMnt content of 7% (Fig. 13d_1, 13d_2, 13d_3, 13d_4, and 13d_5) or 9% (Fig. 13e_1, 13e_2, 13e_3, 13e_4, and 13e_5) were similar to that with OMnt content of 3% (Fig. 13b_1, 13b_2, 13b_3, 13b_4, and 13b_5).

The EIS curves of OMnt/EP composite membranes with different thicknesses of 0.08, 0.12, 0.14, 0.18 and 0.20 mm when their OMnt contents of 1%, 3%, 5%, 7%, and 9% are shown in Fig. 13. From Fig. 13a_1–13e_5, it can be seen that the corrosion resistance of composite membrane with a thickness of 0.18–0.20 mm after it was immersed in NaCl (1.0 mol/L) for one week was much better than that of the composite membrane with a thickness of 0.08–0.14 mm. As the immersing time increased, the corrosion resistance of the composite membrane decreased gradually. When the immersion time was the same, the resistance value of the

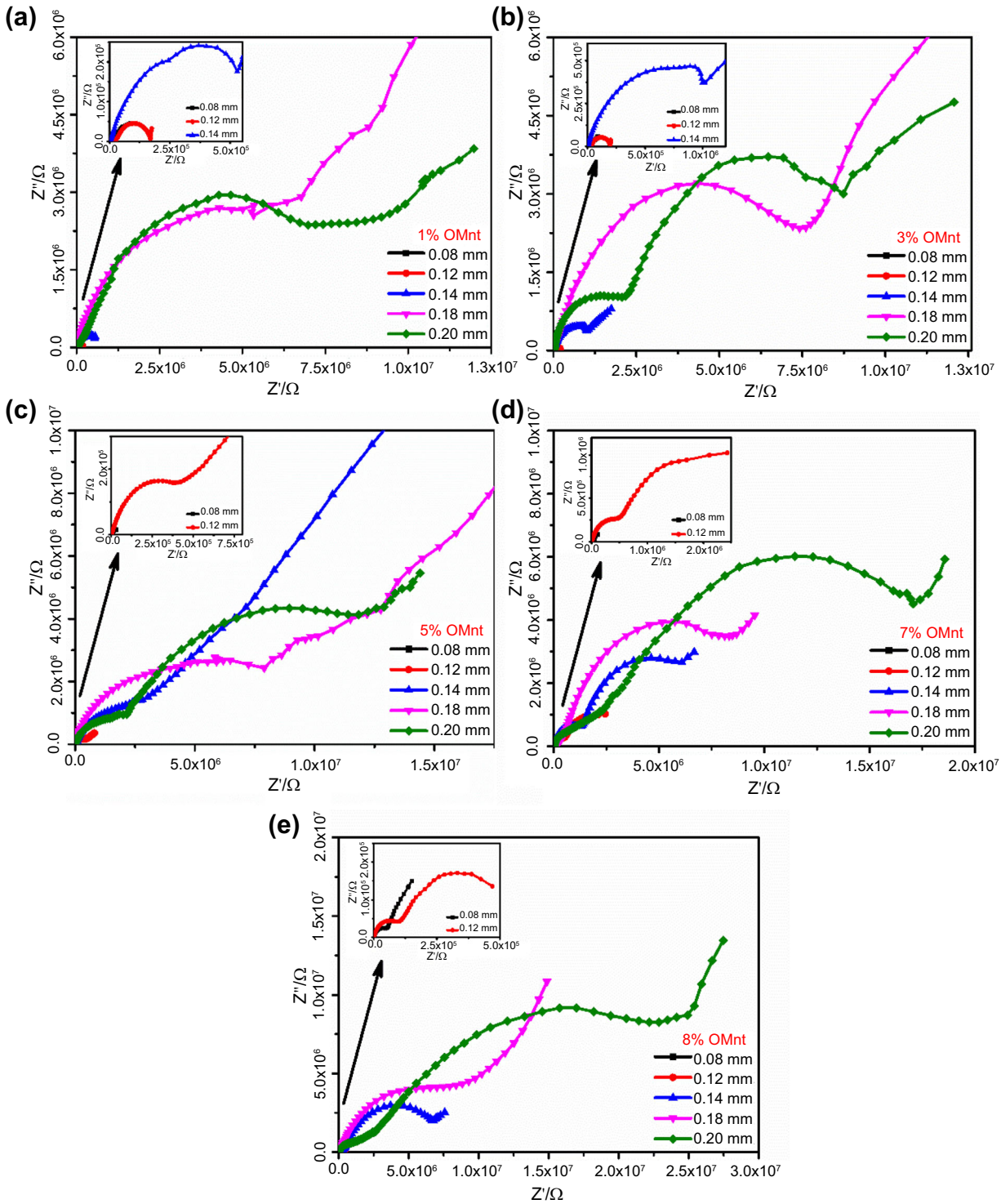

Fig. 12: EIS polarization curves of OMnt/EP composite membrane with different OMnt contents and thicknesses

Table 3: EIS values of OMnt/EP with different OMnt contents and thicknesses

Sample	Membrane thickness/mm	R_{ct}/Ω	Sample	Membrane thickness/mm	R_{ct}/Ω
1% OMnt/EP	0.08	2.42×10^4	7% OMnt/EP	0.08	3.96×10^4
1% OMnt/EP	0.12	1.69×10^5	5% OMnt/EP	0.18	7.79×10^6
1% OMnt/EP	0.14	5.29×10^5	5% OMnt/EP	0.20	1.19×10^7
1% OMnt/EP	0.18	6.51×10^6	7% OMnt/EP	0.12	4.56×10^5
1% OMnt/EP	0.20	8.52×10^6	7% OMnt/EP	0.14	6.06×10^6
3% OMnt/EP	0.08	2.62×10^4	7% OMnt/EP	0.18	8.16×10^6
3% OMnt/EP	0.12	1.96×10^5	7% OMnt/EP	0.20	1.71×10^7
3% OMnt/EP	0.14	1.04×10^6	9% OMnt/EP	0.08	5.19×10^4
3% OMnt/EP	0.18	7.56×10^6	9% OMnt/EP	0.12	4.69×10^5
3% OMnt/EP	0.20	8.56×10^6	9% OMnt/EP	0.14	6.68×10^6
5% OMnt/EP	0.08	3.42×10^4	9% OMnt/EP	0.18	8.40×10^6
5% OMnt/EP	0.12	4.08×10^5	9% OMnt/EP	0.20	2.29×10^7
5% OMnt/EP	0.14	2.89×10^6			

Table 4: The comparison of the impedance of montmorillonite-based composite coatings

Number	Impedance/ Ω	Membrane composition	Corrosive medium	Reference
1	9.40×10^5	Montmorillonite organoclay (OMnt)/epoxy resin (EP) coatings	5 wt% NaCl solution	[23]
2	6.00×10^6	Montmorillonite (Mnt)/2-benzylbenzimi-dazole (2-BBI)/ epoxy resin (EP) coatings	3.5 wt% NaCl solution	[13]
3	9.21×10^4	Montmorillonite (Mnt)/2-acrylamido-2-methyl propane sulfonic acid	3.5 wt% NaCl solution	[12]
4	1.00×10^6	Hybrid clay-organosilane derived sol–gel coatings	1.0 mol/L 2.0 NaCl solution	[5]
5	6.46×10^7	Organo-montmorillonite (Cloisite 30B)/epoxy resin (EP) coatings	3.5 wt% NaCl solution	[22]
6	1.34×10^9	Clay/phosphate/epoxy (CPE) nanocomposites coatings	0.5 mol/L HCl solution	[9]
7	2.29×10^7	Organo-nanomontmorillonite/epoxy resin (OMnt/EP)	1.0 mol/L 2.0 NaCl solution	This work

composite membrane increased along with the thickness of the composite membrane, which is consistent with that in Fig. 12.

Adhesion test

The adhesion of pure EP membrane and OMnt/EP membrane coated on the surface of aluminum plate were tested according to Chinese Adhesion Test standard (GB/T 9286-1998) and the results are shown in Fig. 14, which clearly shows that there was no obvious difference in shedding phenomenon at the intersection of the scratches on the surface of the above membranes. This indicates that pure EP membrane and OMnt/EP composite membrane have same binding force with the surface of the aluminum plate, which may be due to a synergistic effect between OMnt and EP in the membrane that reduced micropores and cracks in their composite membrane.

Conclusions

1. The corrosion potential of OMnt-EP composite membrane was positively shifted by 0.04 V and its

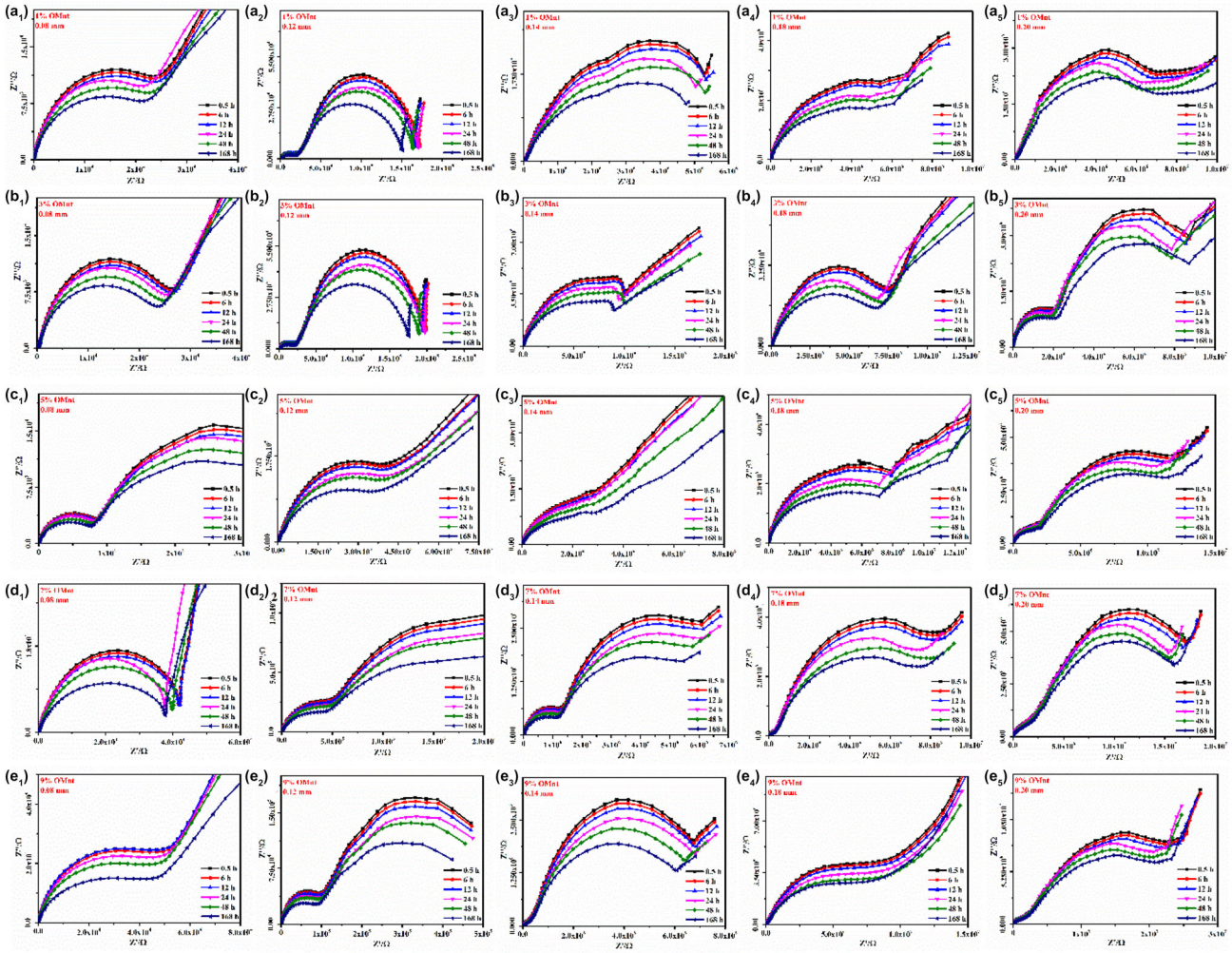

Fig. 13: EIS polarization curves of OMnt/EP composite membrane with 1%, 3%, 5%, 7%, and 9% OMnt contents and different thicknesses at the time interval of 0.5, 6, 12, 24, 48, and 168 h

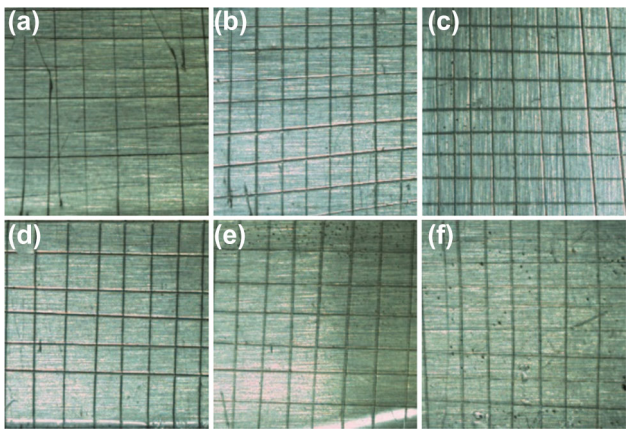

Fig. 14: Adhesion test results of pure EP (a) and EP/OMnt composite membranes with different contents of OMnt 1% (b), 3% (c), 5% (d), 7% (e), and 9% (f) on aluminum plate surface

current density was reduced by at least three orders of magnitude compared to that of aluminum plate. In detail, the corrosion potential of OMnt-EP membrane increased along with its OMnt content, while its current density decreased along with its OMnt content.

2. The impedance of OMnt-EP composite membrane increased along with its OMnt content. The addition of OMnt into EP increased its impedance, and both the amount of OMnt and thickness of the membranes had positive effects on its corrosion resistance.
3. The addition of OMnt and nano-sized Mnt into EP did not change the adhesion force between the composite membrane and surface of aluminum plate but enhanced the anticorrosion performance of the composite membrane and reduced its corrosive rate. Both its OMnt content and thickness had positive impacts on its anticorrosion performance.

Acknowledgments The authors would like to thank the financial support from the National Natural Science Foundation of China (Nos. 21173193 and 21301154), the Zhejiang provincial natural science foundation (No. LQ19B010002), and Engineering Research Center of Non-metallic Minerals of Zhejiang Province (ZD2020K08).

Conflict of interest The authors declare that they have no conflict of interest.

References

1. Zabihi, O, Ahmadi, M, Nikafshar, S, Preyeswary, KC, Naebe, M, ''A Technical Review on Epoxy-Clay Nanocomposites: Structure, Properties, and Their Applications in Fiber Reinforced Composites.'' *Compos. B Eng.*, **135** 1–24 (2018)
2. Jiang, M, Wu, L, Hu, J, Zhang, J, ''Silane-Incorporated Epoxy Coatings on Aluminum Alloy (AA2024). Part 1: Improved Corrosion Performance.'' *Corros. Sci.*, **92** 118–126 (2015)
3. Jiang, M, Wu, L, Hu, J, Zhang, J, ''Silane-Incorporated Epoxy Coatings on Aluminum Alloy (AA2024). Part 2: Mechanistic Investigations.'' *Corros. Sci.*, **92** 127–135 (2015)
4. Piazza, D, Lorandi, NP, Pasqual, CI, Scienza, LC, Zattera, AJ, ''Influence of a Microcomposite and a Nanocomposite on the Properties of an Epoxy-Based Powder Coating.'' *Mater. Sci. Eng. A*, **528** (22–23) 6769–6775 (2011)
5. Fedel, M, Callone, E, Diré, S, Deflorian, F, Olivier, MG, Poelman, M, ''Effect of Na-Montmorillonite Sonication on the Protective Properties of Hybrid Silica Coatings.'' *Electrochim. Acta*, **124** 90–99 (2014)
6. Ji, W, Li, C, Huang, W, Yu, H, Chen, R, Yu, Y, Yeh, JM, Tang, WC, Su, YC, ''Composite Coating with Synergistic Effect of Biomimetic Epoxy Thermoset Morphology and Incorporated Superhydrophobic Silica for Corrosion Protection.'' *Express Polym. Lett.*, **10** (11) 950–963 (2016)
7. Viroulaud, R, Swiatowska, J, Seyeux, A, Zanna, S, Tardelli, J, Marcus, P, ''Influence of Surface Pretreatments on the Quality of Trivalent Chromium Process Coatings on Aluminum Alloy.'' *Appl. Surf. Sci.*, **423** 927–938 (2017)
8. Zhu, W, Li, W, Mu, S, Fu, N, Liao, Z, ''Comparative Study on Ti/Zr/V and Chromate Conversion Treated Aluminum Alloys: Anticorrosion Performance and Epoxy Coating Adhesion Properties.'' *Appl. Surf. Sci.*, **405** 157–168 (2017)
9. Deyab, M, Hamdi, N, Lachkar, M, Bali, B, ''Clay/Phosphate/Epoxy Nanocomposites for Enhanced Coating Activity Towards Corrosion Resistance.'' *Prog. Org. Coat.*, **123** 232–237 (2018)
10. Bari, GAKMR, Park, S, Parveen, AS, Lee, S, Kim, H, ''High Barrier Performance of the Multilayer Film Based on Epoxy and Montmorillonite.'' *Prog. Org. Coat.*, **126** 1–7 (2019)
11. Piazza, D, Lorandi, NP, Pasqual, CI, Scienza, LC, Zattera, AJ, ''Polyester-Based Powder Coatings with Montmorillonite Nanoparticles Applied on Carbon Steel.'' *Prog. Org. Coat.*, **73** (1) 42–46 (2012)
12. Atta, AM, El-Saeed, AM, Al-Lohedan, HA, Wahby, M, ''Effect of Montmorillonite Nanogel Composite Fillers on the Protection Performance of Epoxy Coatings on Steel Pipelines.'' *Molecules*, **22** (6) 905 (2017)
13. Mehrabian, N, Dariani, AAS, ''Anticorrosive Performance of Epoxy/Modified Clay Nanocomposites.'' *Polym. Compos.*, **39** E2134–E2142 (2018)
14. Wang, N, Cheng, KO, Wu, H, Wang, C, Wang, QC, Wang, FH, ''Effect of Nano-Sized Mesoporous Silica MCM-41 and MMT on Corrosion Properties of Epoxy Coating.'' *Prog. Org. Coat.*, **75** (4) 386–391 (2012)
15. Minisini, B, Rolère, S, Coulon, JF, Poncin-Epaillard, F, ''Influence of the Chemical Composition and Formulation of Fluorinated Epoxy Resin on Its Surface Characteristics.'' *Eur. Polym. J.*, **112** 452–460 (2019)
16. Visser, P, Terryn, H, Mol, JMC, ''On the Importance of Irreversibility of Corrosion Inhibitors for Active Coating Protection of AA2024-T3.'' *Corros. Sci.*, **140** 272–285 (2018)
17. Dong, Y, Ma, L, Zhou, Q, ''Effect of the Incorporation of Montmorillonite-Layered Double Hydroxide Nanoclays on the Corrosion Protection of Epoxy Coatings.'' *J. Coat. Technol. Res.*, **10** (6) 909–921 (2013)
18. Ghanbari, A, Attar, MM, ''A Study on the Anticorrosion Performance of Epoxy Nanocomposite Coatings Containing Epoxy-Silane Treated Nano-silica on Mild Steel Substrate.'' *J. Ind. Eng. Chem.*, **23** 145–153 (2015)
19. Krupskaya, VV, Zakusin, SV, Tyupina, EA, Dorzhieva, OV, Chernov, MS, Bychkova, YV, ''Transformation of Structure and Adsorption Properties of Montmorillonite Under Thermochemical Treatment.'' *Geochem. Int.*, **57** (3) 314–330 (2019)
20. Huttunen-Saarivirta, E, Vaganov, GV, Yudin, VE, Vuorinen, J, ''Characterization and Corrosion Protection Properties of Epoxy Powder Coatings Containing Nanoclays.'' *Prog. Org. Coat.*, **76** 757–767 (2013)
21. Tomić, M, Dunjić, B, Nikolić, MS, Maletaškić, J, Pavlović, VB, Bajat, J, Djonlagić, J, ''Dispersion Efficiency of Montmorillonites in Epoxy Nanocomposites Using Solution Intercalation and Direct Mixing Methods.'' *Appl. Clay Sci.*, **154** 52–63 (2018)
22. Bagherzadeh, MR, Mousavinejad, T, ''Preparation and Investigation of Anticorrosion Properties of the Water-Based Epoxy-Clay Nanocoating Modified by Na^+-Mnt and Cloisite 30B.'' *Prog. Org. Coat.*, **74** (3) 589–595 (2012)
23. Nematollahi, M, Heidarian, M, Peikari, M, Kassiriha, SM, Arianpouya, N, Esmaeilpour, M, ''Comparison Between the Effect of Nanoglass Flake and Montmorillonite Organoclay on Corrosion Performance of Epoxy Coating.'' *Corros. Sci.*, **52** (5) 1809–1817 (2010)
24. Moradi, M, Yeganeh, H, Pazokifard, S, ''Synthesis and Assessment of Novel Anticorrosive Polyurethane Coatings Containing an Amine-Functionalized Nanoclay Additive Prepared by the Cathodic Electrophoretic Deposition Method.'' *RSC Adv.*, **6** (33) 28089–28102 (2016)
25. Wang, L, Jian, X, Yuan, J, Ren, L, Zhang, K, ''Preparation of Epoxy-Montmorillonite Nanocomposite and Its Formation Mechanism.'' *J. Dalian Univ. Technol.*, **40** (6) 681–684 (2000)